Ultrasound Imaging of Brain Shunts

Project Final Report

600.446 Advanced Computer Integrated Surgery Spring 2013

Team 1

Members: Yang Hong, Rongguang Han

Mentors: Dr. Emad Boctor, Dr. Russell Taylor

Johns Hopkins University

Abstract. High incidence of occlusions in brain shunt motivates the developing of easy and fast clearing system for the shunt revision. One problem needs to solve is the visualization of the clearing results. In this project, we proposed a method to image the occlusion in brain shunts through the skull using external ultrasound transducer probe, together with photoacoustic (PA) excitation. Feasibility of the methods has been demonstrated with PVA-C brain phantom and fresh bones of different thickness. Different levels of occlusions and distance between the fiber end point and the occlusion can be detected and distinguished from the output images.

Key words: human brain imaging, ultrasound imaging, photoacoustic excitation, brain shunts, phantom

1. Introduction

The most common treatment for hydrocephalus is to place a cerebrospinal fluid (CSF) shunt to divert excess CSF to a re-absorption site and regulate the intracranial pressure. However, CSF shunts have an unacceptably high incidence of occlusions from in-grown tissues. Our project is to explore ultrasound imaging, together with photoelectric excitation to image the occlusions and brain shunts, so a system of minimally invasive clearing of the brain shunts could be further developed.

In the first stage of this project, we show that PA excitation can be used for the occlusion imaging. In the second stage, we demonstrate the signals generated by PA excitation can be detected through the

skull, which makes it possible to use the external ultrasound probe. In the last stage, we propose a method to visualize the relative position of the occlusion and a delayed method to monitor the clearing procedure.

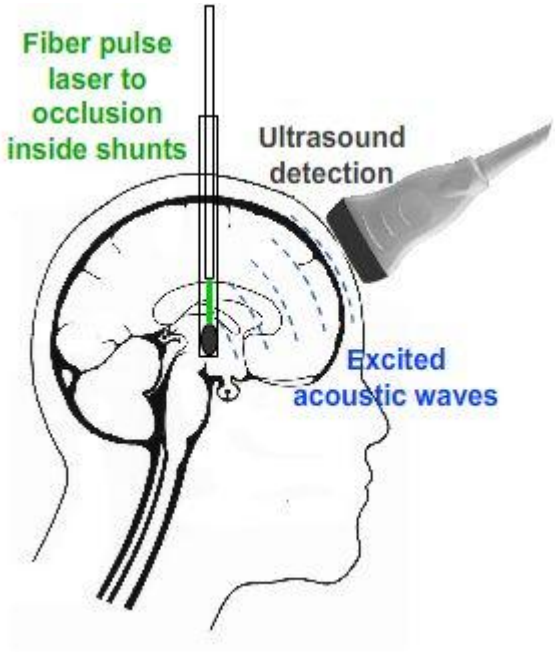

Figure 1: Illustration of the method to image the occlusion inside the skull with PA imaging

1.1 Motivation

Hydrocephalus is caused by excessive CSF accumulates in the ventricular space, creating increased pressure on the brain. Pressure distends ventricles and can lead to death. Until now, no medical therapy to treat hydrocephalus exists. The only effective treatments are surgical. Among all the surgical solutions, the most common one for hydrocephalus is to place a cerebrospinal fluid (CSF) shunt into the ventricular system of the brain, to divert excess CSF to a re-absorption site and regulate the intracranial pressure. A valve within the shunt regulates the flow of CSF. The shunt procedure is performed by a neurosurgeon. Shunts can become clogged or malfunction and surgical revisions are often required. Over 40,000 shunt-related operations are performed annually in US (one every 15 minutes), but only 30% are the patient's first surgery to treat hydrocephalus.

This unacceptably high incidence of occlusions is from in-grown tissues like choroid plexus, connective tissue, neurogliosis and blood, which block CSF flow. Failure rates are estimated to be around 40% in the first year and 80%within 10 years. Currently, the only clinical solution for resolving obstructions is either shunt replacement or revision. If removal of malfunctioning shunt

presents hemorrhage risk, the shunt is left and new shunt placed. Though placement of the shunt is a very safe procedure today, certain risks still exist. For example, bleeding in the brain, damage to brain, drug reaction and anesthesia reaction. And the shunt revision surgery will make the patients face these risks again.

Now, shunt-clearing system is under developed to minimize the surgery risks and the surgery time of shunt revision. To help monitor the clearing process or at least monitor the clearing results, an imaging auxiliary device is needed. The specific aim of this project is to propose a technical method and demonstrate its validation, which can image the occlusions in the brain shunt.

1.2 Background

Ultrasonography is an ultrasound-based diagnostic imaging technique widely used for visualizing body structures including tendons, muscles, joints, vessels and internal organs for possible pathology or lesions. However, ultrasonography devices have trouble in penetrating bone. Also, the depth penetration of ultrasound is limited depending on the frequency of imaging. Thus, ultrasound imaging itself is a very limited technique for this project since the existence of the skull.

Photoacoustic (PA) imaging, which is based on the photoacoustic effect, possessing many attractive characteristics such as the use of nonionizing electromagnetic waves, good resolution and contrast, portable instrumentation, and the ability to partially quantitate the signal, has been developed extensively over the last decade. It was first discovered by Alexander Graham Bell in 1880. Electromagnetic (light) waves are converted to acoustic waves due to absorption and thermal excitation. The photoacoustic effect has been previously exploited to lead to the invention of photoacoustic spectroscopy and is currently used in biomedical applications such as structural imaging, functional imaging, and molecular imaging.

By launching high frequency pulses of light onto a medium, the energy of the light is absorbed and converted into heat, which makes the molecules become thermally excited. Then the pressure variations caused by radiation of the heat will propagate as ultrasound waves in the medium. So that it can be detected by acoustic devices such as ultrasound probe.

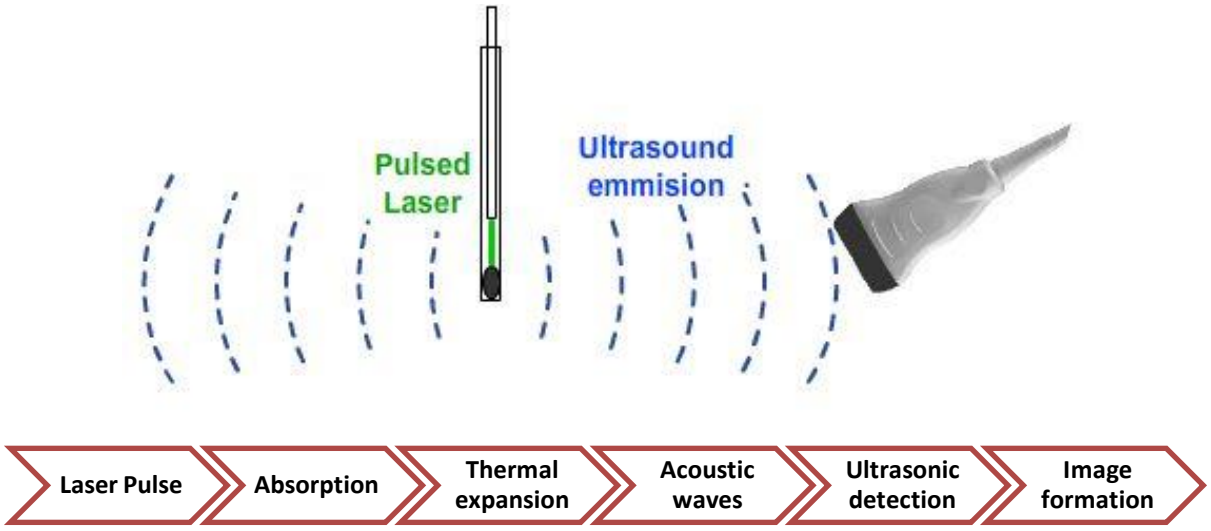

Figure 2: Mechanism of photoacoustic imaging

1.3 Significance

This project proposes a new method to image the occlusion in the shunt through the skull, so that the shunt revision surgery procedure can be monitored in a delayed way and the clearing results can also be verified, which will support the shunt-clearing system being further developed. This approach also shows a promising future research direction with photoacoustic imaging through human skull, which was limited by the high attenuation of the skull in the traditional ultrasound imaging system.

2. Technical approach

2.1 Phantom Construction

This project is to develop a new technology that can be used for the Ventricular Brain Shunts. A phantom, that can mimic the ultrasound properties of human brain, needs to be prepared for the investigation. For the purpose of minimizing the cost, our group decides to build our own phantom. Several papers have been investigated and studied. Finally, two of them are selected and used as the guide to build the phantom for the brain part and the skull part, respectively.

2.1.1 Brain Phantom

For the brain part, we choose the polyvinyl alcohol cryogel (PVA-C) as the main building material.

But before the PVA-C based phantom is constructed due to the temporary unavailability of the material, a jello based phantom is constructed for the preliminary test. The results can also be used to compare with the PVA-C phantom.

PVA-C is a typical tissue-mimicking material for ultrasound imaging. It is formed from PVA solution undergoing some freeze-thaw (F/T) cycles. As the optical and mechanical properties change with the number of F/T cycle, certain requirements, like the scattering coefficient and absorption coefficient, for the phantom can be achieved. This kind of phantom can be used in a permanent way under humidity-controlled conditions.

The construction process is specified below:

1) 5% or 8% of PVA by weight are dissolved in distilled water.
2) The solution is transferred to the oven for about 7 hours at the temperature of 93 degree Celsius.
3) The PVA solution is cooled to -17 degree Celsius for about 12 hours.
4) The solution warms back to room temperature in a continuous way for another 12 hours.

Step 1) to 4) is a whole F/T cycle. If needed, this F/T cycle can be repeated for several times. Without the addition of dimethyl sufoxide, the scattering coefficient will increase with each cycle and the phantom will be stiffer, too.

After some tests and comparing with the data in [1], we used the 6% PVA solution at 1 F/T cycle for our project.

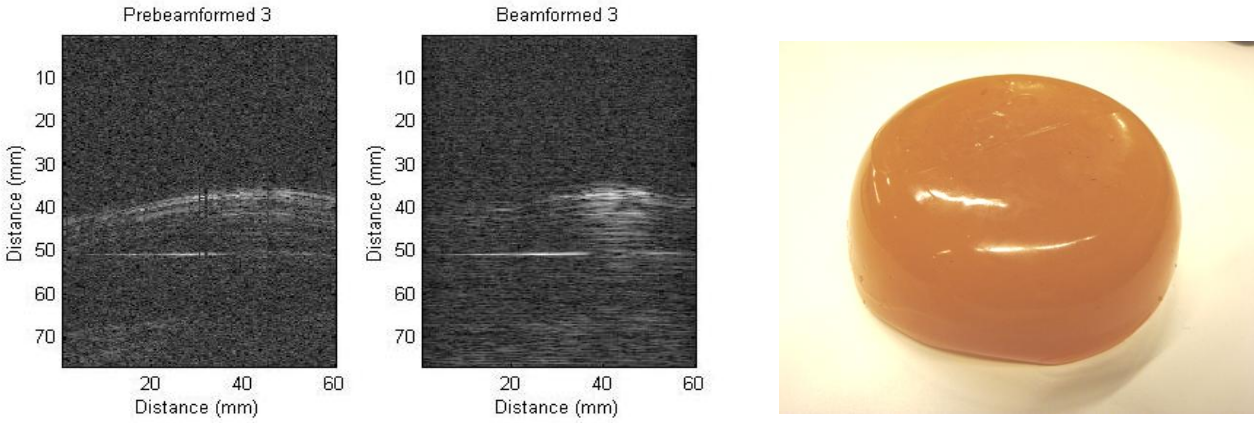

Firgue 3: PA delayed image (left) using PA excitation for Jello based phantom (right)

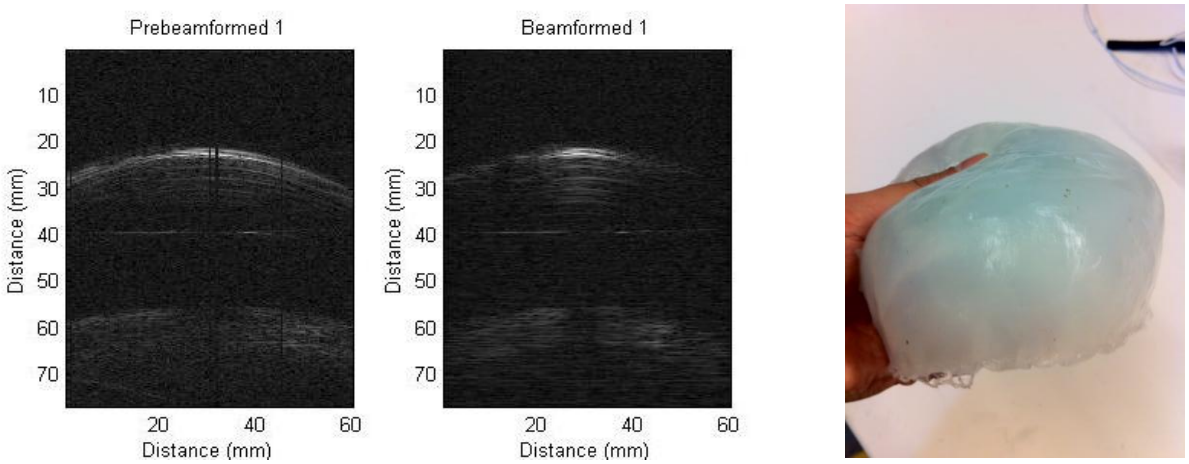

Firgue 4: PA delayed image (left) using PA excitation for PVA-C based phantom (right)

From figure 3 and figure 4, we can see that the PVA-C based phantom is relatively softer than the Jello based one, which is more like the real human brain texture. The PVA-C based phantom is a better choice for this project can be found in ref [2]. Also, the delayed images getting from the same system setup showed that PVA-C based phantom has a better contrast than the Jello based phantom. The results we presented in Section 3 are all obtained with the PVA-C phantom. A brain shaped PVA-C phantom has also been built in Figure 5, the experiment results using which does not change much actually.

Figure 5: Brain shaped PVA-C phantom

2.1.2 Skull Phantom

In order to explore the occlusion in the shunt by using the external ultrasound probe to detect the signals through the human skull, a good phantom that can mimic the acoustical and optical properties is preferred. In this project, we designed the skull phantom construction process based on a medical modeling process by using the 3DP technology from ref [3].

The typical construction process is specified below:

1) Use CT/MRI to get the medical image
2) 3D model reconstruction in the medical software
3) Computer Aided Design
4) STL file generation
5) Prototyping (Powder-binder combination of ZP130^{TM} and ZB58^{TM} are used on the Z510^{TM} Spectrum 3D printer.)
6) Post-processing: cleaning, support removal, infiltration, etc.

In step 6), the infiltration is performed by immersion under vacuum conditions in a dedicated chamber. The samples were maintained at -95kPa for min, at the temperature of $25°C$. Then, the atmospheric inlet valve is opened to relieve the vacuum, causing a further penetration of the infiltrant by atmospheric pressure action. Finally, the samples are extracted from the chamber and the excess resin is wiped off the surface.

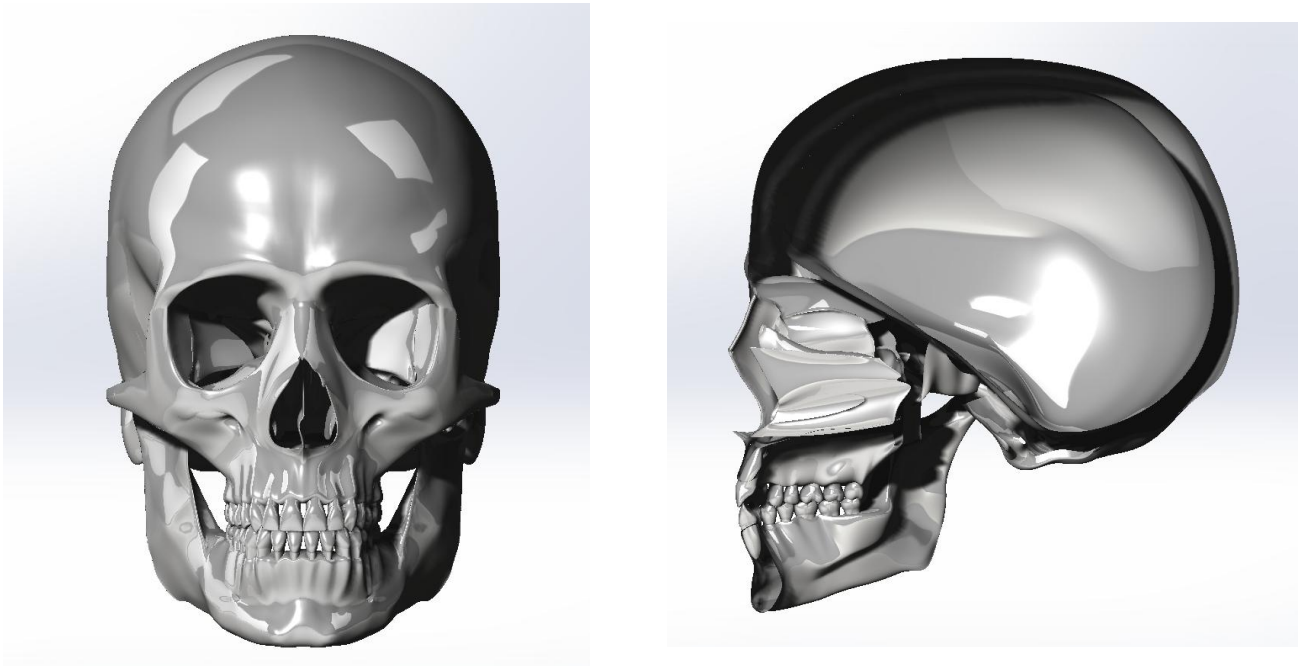

Figure 6: 3D model for the skull phantom (created in Solidworks)

Figure 6 shows the 3D model created in the Solidworks for the skull phantom. This can be used to generate the STL file and finally used in the 3D printer for the skull. Though, we finally choose to use a piece of real bone from a pig to do our experiment due to the unavailability of the specific 3D

printer, this model still has its value for the further work.

2.2 System setup

The Photoaoustic Laser System of OPOTEK Inc. has been used to project pulses at 1064nm wavelength into a fiber of 1mm diameter, which has been inserted into the shunts with its tip directly pointing to the occlusion material. SonixTouch ultrasound system, developed by Ultrasonix Medical Corporation (Richmond, Canada), was used to detect the excited acoustic waves, together with a transducer probe placed right on top of the phantom. The Sonix DAQ device, jointly developed by the University of Hong Kong and Ultrasonix, was used to collect the pre-beamformed radiofrequency (RF) data from the US machine into .daq files. Finally, those .daq files are processed with MATLAB to get the beamformed image.

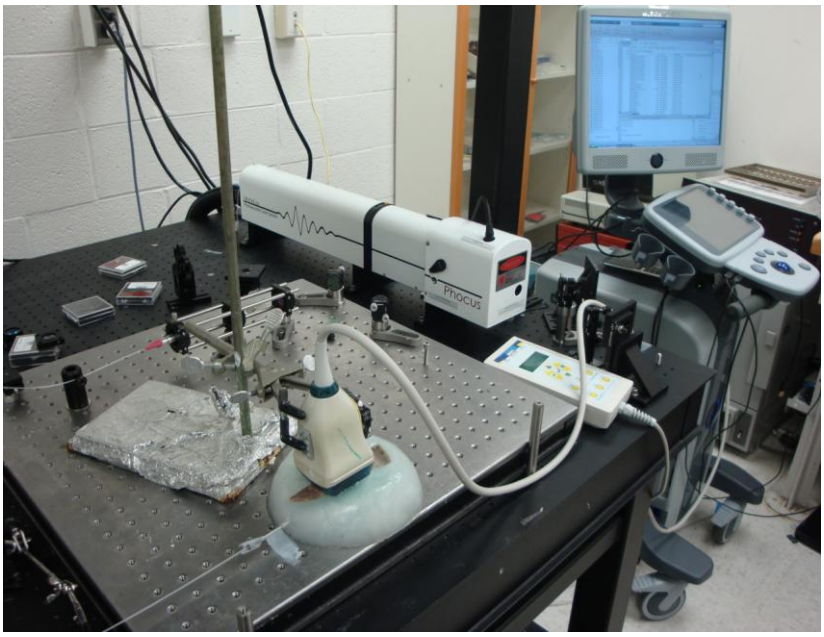

Figure 7: System setup

2.3 Experimental setup

A shunts mimicking plastic tube containing water and occlusion has been inserted into the brain phantom horizontally. The transducer probe has been put in aligned with the shunt. Figure 8 shows a B-mode ultrasound image of the shunts inside the phantom, with fiber and occlusion inserted. Though we cannot see the fiber and the occlusion in the shunts clearly, their positions can be decided by the shadows they have created below them.

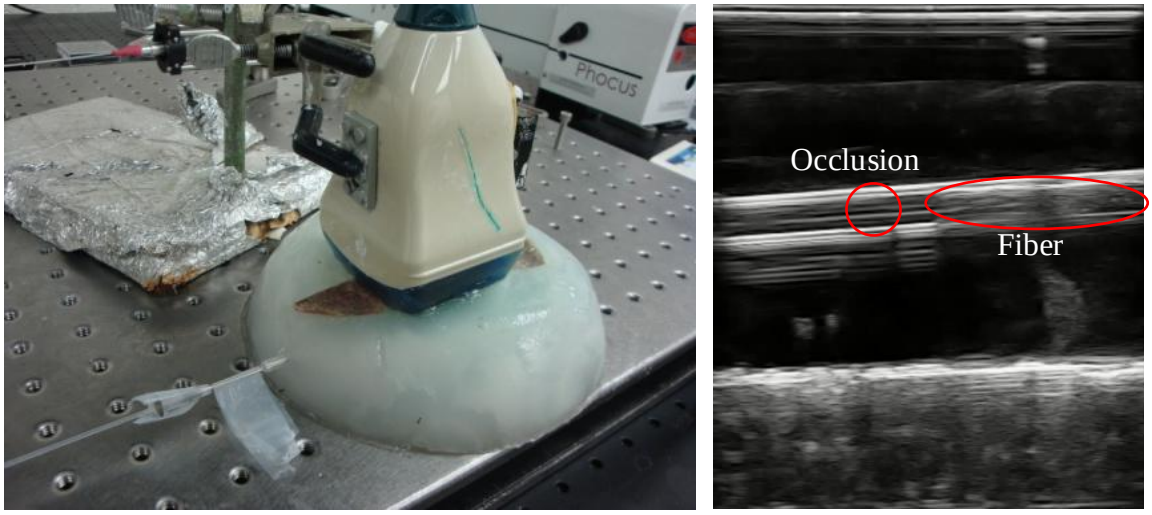

Figure 8: Shunt with fiber and occlusion in the phantom (left) and its B-mode image (right)

High attenuation jello-based material has been used to mimic the occlusion. Nova of Ophir Optronics has been used as the laser energy/power meter. Energy between 0.7mJ/cm^2 to 1.5mJ/cm^2 at the fiber end tip has been adopted for the experiments, which is much lower than the maximum allowable energy of 30mJ/cm^2 exposed on tissue according to the ISO laser safety standards. A limitation of our occlusion material is that it will get burnt when the laser energy is over 1mJ/cm^2, and no signal will be generated after that. A brachytherapy seed has been put right before the occlusion material to prevent this situation when high energy is needed in the experiments of visualization of the fiber end point. The occlusion at the end of the shunt is used to prevent water from leaking out, which is far out of the FOV.

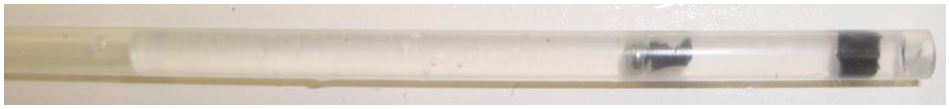

Figure 9: Shunts with water, brachytherapy seed and occlusion inside

Different sizes of the occlusion material have been prepared for imaging in Figure 10. The thickness is halved for the second occlusion.

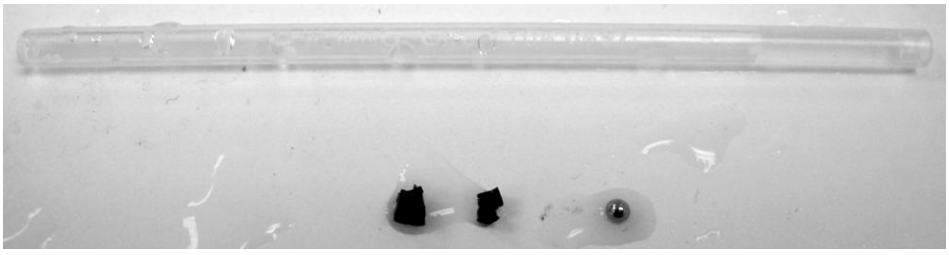

Figure 10: Different sizes of occlusions

To mimic human skull, a fresh pig pelvis bone has been cut and shaved into two pieces of different thickness, 2mm and 4mm. Then, one of the two pieces has been inserted between the phantom and the transducer probe.

In the experiments to visualize fiber end point, a metal needle has been tied up together with the fiber, and a piece of occlusion material has been put at the end of the needle. The acoustic wave generated by the seed and the occlusion will be reflected by that piece of occlusion material, so the position of the fiber end point can be seen in PA images.

Figure 11: Fiber tied up together with needle and a piece of occlusion material

To mimic the reversed process of clearing the shunts, occlusion material has been cut into tiny pieces and mixed with ultrasound jell to put into a injection syringe and inject into the shunts. Therefore, visualization of the accumulation of the occlusion could be achieved.

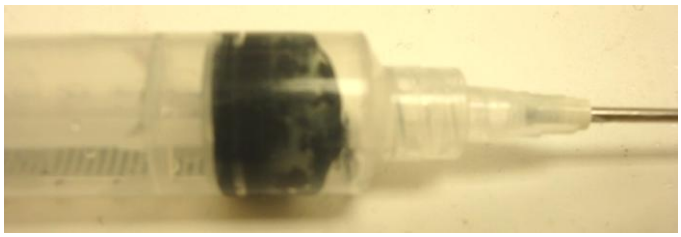

Figure 12: Syringe with tiny pieces of occlusion material and mixed with ultrasound jell

3. Results & Discussion

3.1 Visualization of occlusion without skull

With fiber end point energy larger than 0.3mJ/cm^2, the visualization of occlusion without skull can be achieved and shown in Figure 13. The distance between the fiber end point and the occlusion is 2mm in this experiment.

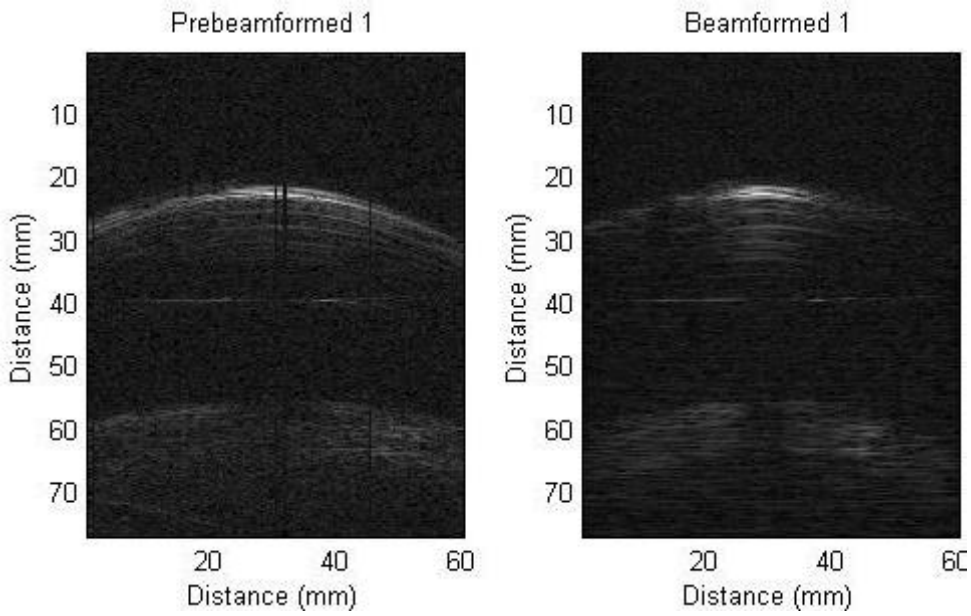

Figure 13: PA image of occlusion in PVA-C brain phantom without skull

To eliminate the probability that we are seeing the fiber's end point other than the occlusion, PA image with no occlusion has been collected in Figure 14. No photoacoustic signal can be generated, so nothing can be seen in the output image. This also represents the initial condition when the fiber end point is too far away from the occlusion or the final condition of the clearing.

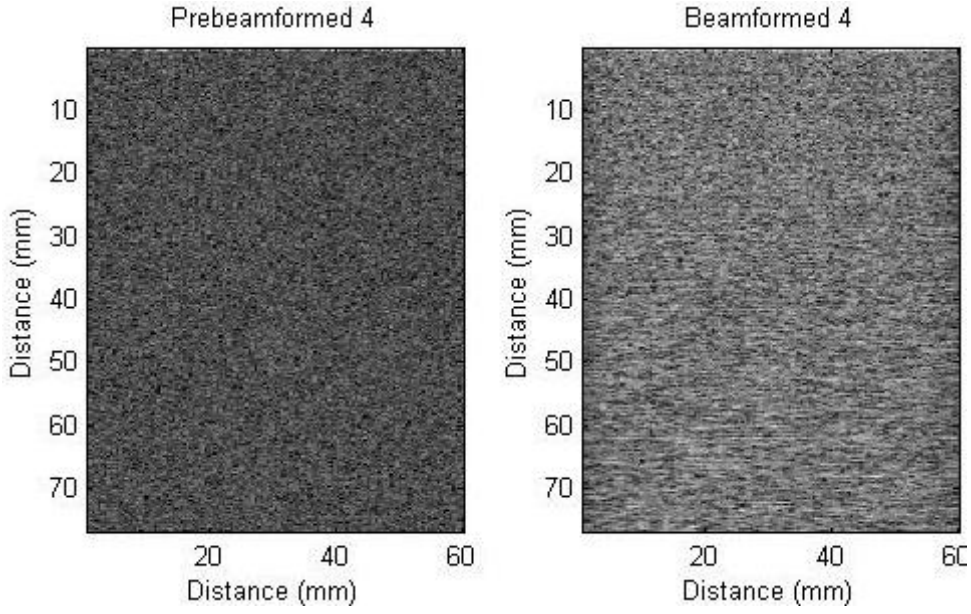

Figure 14: PA image with no occlusion

3.2 Visualization of occlusion with skull

After inserted a piece of 2mm pig bone between the brain phantom and the transducer, B-mode

ultrasound image has been collected and shown in Figure 15.

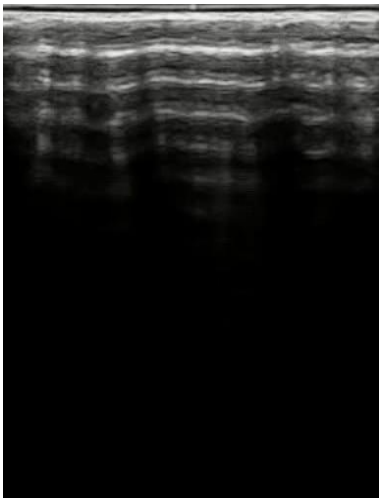

Figure 15: B-mode ultrasound image with 2mm pig bone

All the ultrasound energy has been absorbed by the bone and nothing can be seen behind it. As we all know, ultrasound could go through human skull and provide a highly defocused image. Thus, we can conclude that the pig bone used in our experiments has higher attenuation than real human skull. If we can get PA image with the pig bone, we will definitely get PA image with real human skull with better intensity and resolution.

Fiber end point energy of 0.8mJ/cm2 has been used for the following experiments in this section. PA image of the occlusion with the 2mm piece of bone is shown in Figure 16, and 4mm bone in Figure 17.

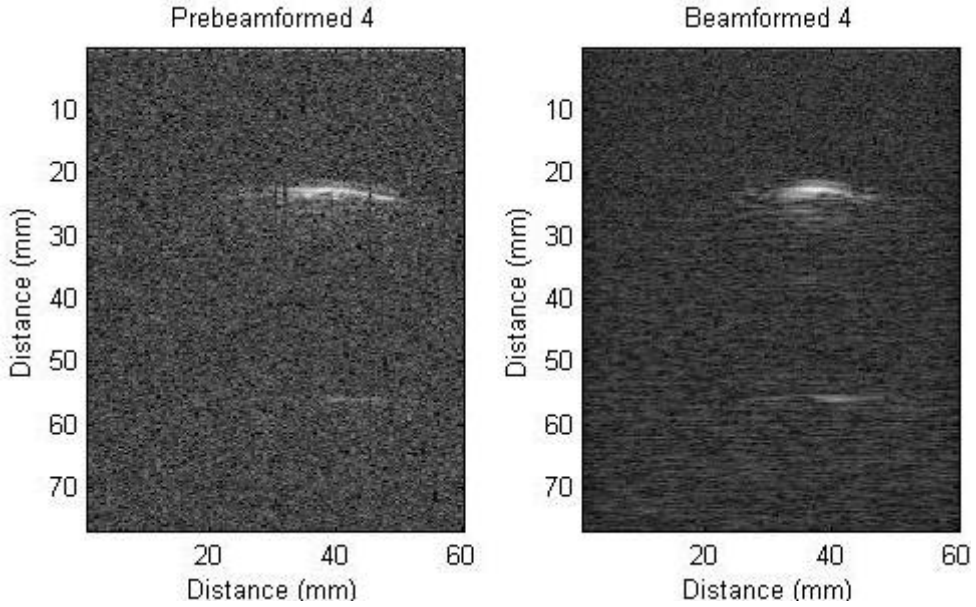

Figure 16: PA image with 2mm pig bone

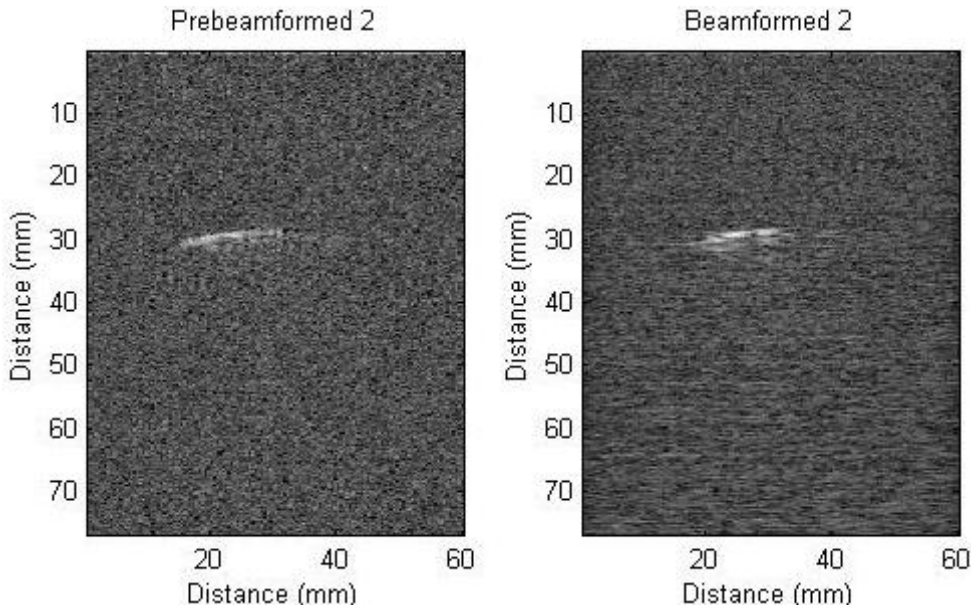

Figure 17 PA image with 4mm pig bone

As we have expected, when the thickness of the bone increases, the occlusion in the output PA image will have lower intensity and contrast.

3.2.1 Experiments with distance between the fiber end point and the occlusion

In previous experiments, the distance between the fiber end point and the occlusion is 2mm. We changed it to 5mm and 10mm, the collected images is shown in Figure18 and Figure 19.

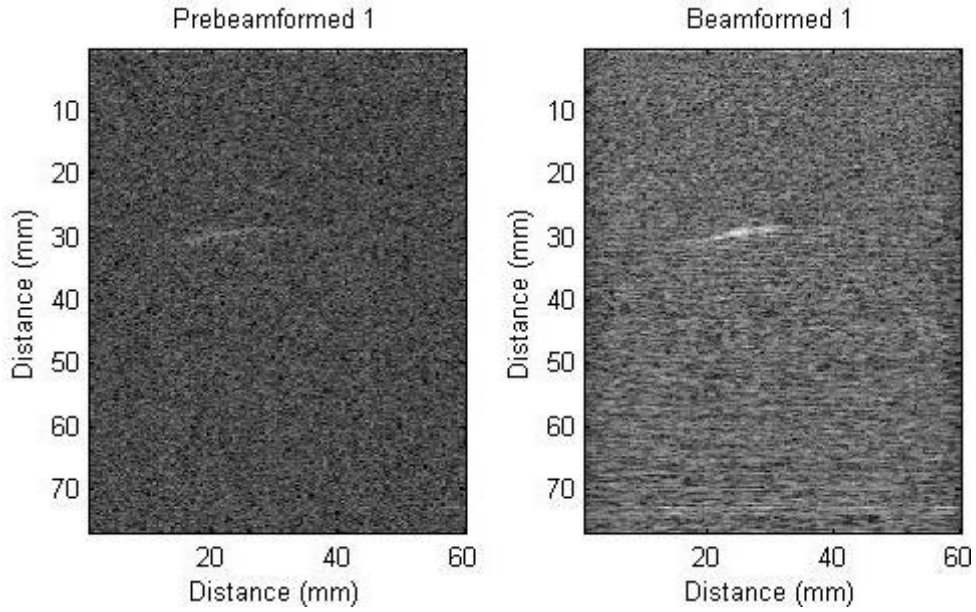

Figure 18: PA image of 5mm between the fiber end tip and the occlusion with 4mm pig bone

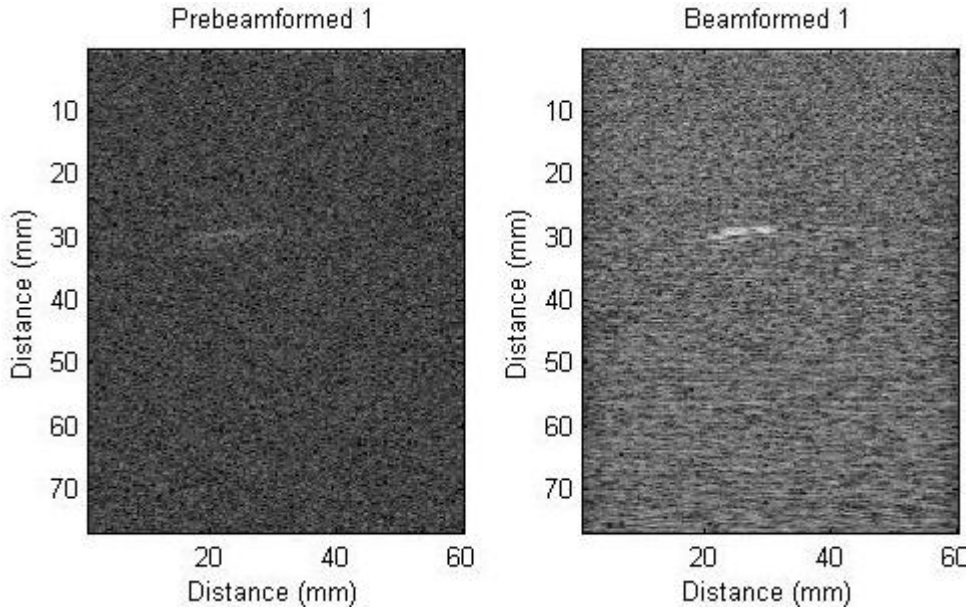

Figure 19: PA image of 10mm between the fiber end tip and the occlusion with 4mm pig bone

From the above figures, we can conclude that, as fiber approaching the occlusion, the intensity and the contrast of the occlusion will increase.

3.2.2 Experiments with different occlusion size

Again we change the distance back to 2mm and double the thickness of the occlusion, the result is shown in Figure 20.

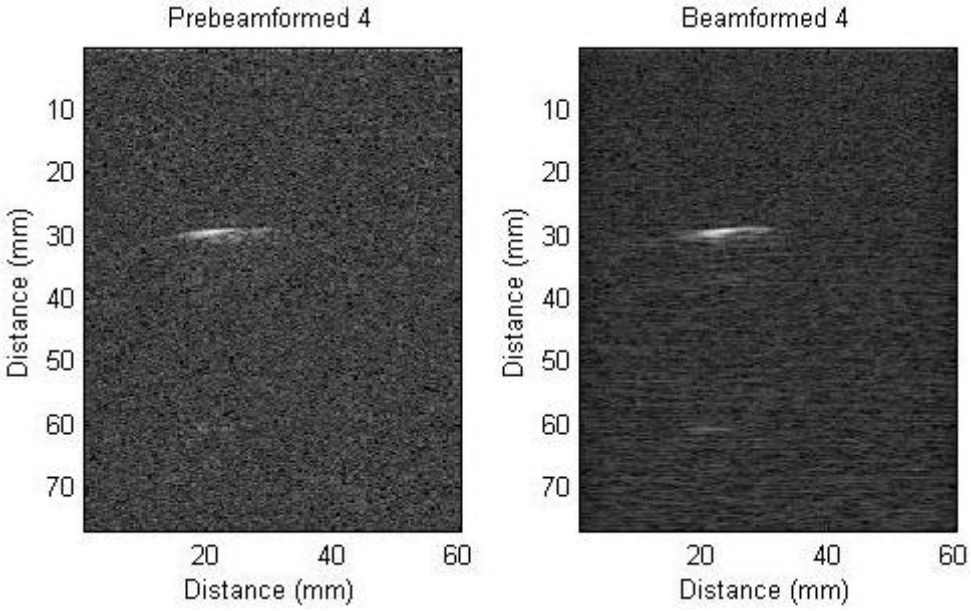

Figure 20: PA image of occlusion of double thickness with 4mm pig bone

As the size of the occlusion increases, the intensity and the contrast of the occlusion will increase.

This is due to that more acoustic wave has been generated, which leads to larger energy detected by each transducer element.

3.3 Visualization of fiber end point

Fiber end point energy 1.2mJ/cm^2 has been used in this experiment. The center of the occlusion material attached with the needle is 3mm before the fiber end point to prevent it from burnt by the fiber. The brachytherapy seed has been put right before the occlusion. The PA image of the fiber approaching the occlusion without skull is shown in the following figures. A short video has been made as well.

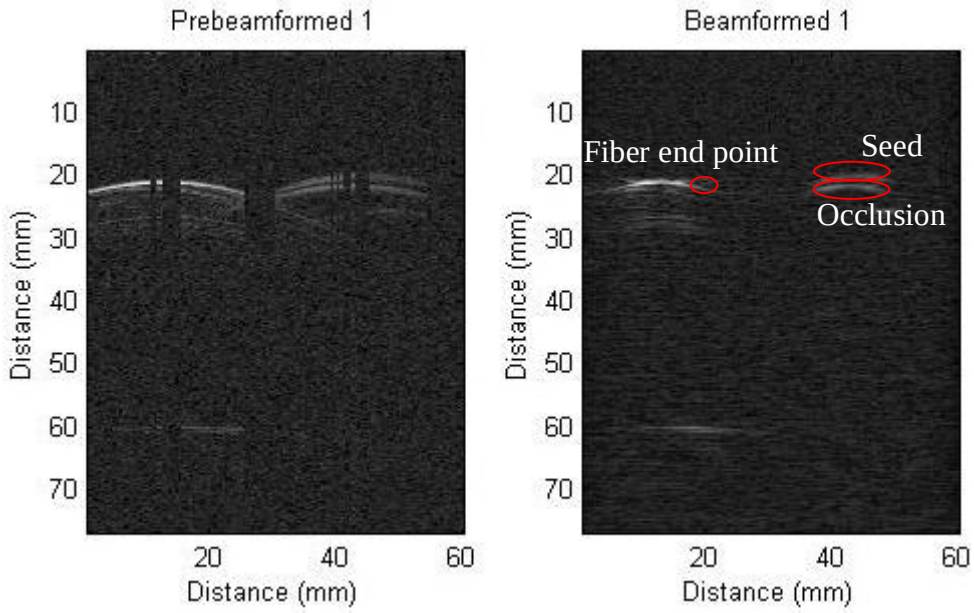

Figure 21: PA image of occlusion and fiber end point at 20mm

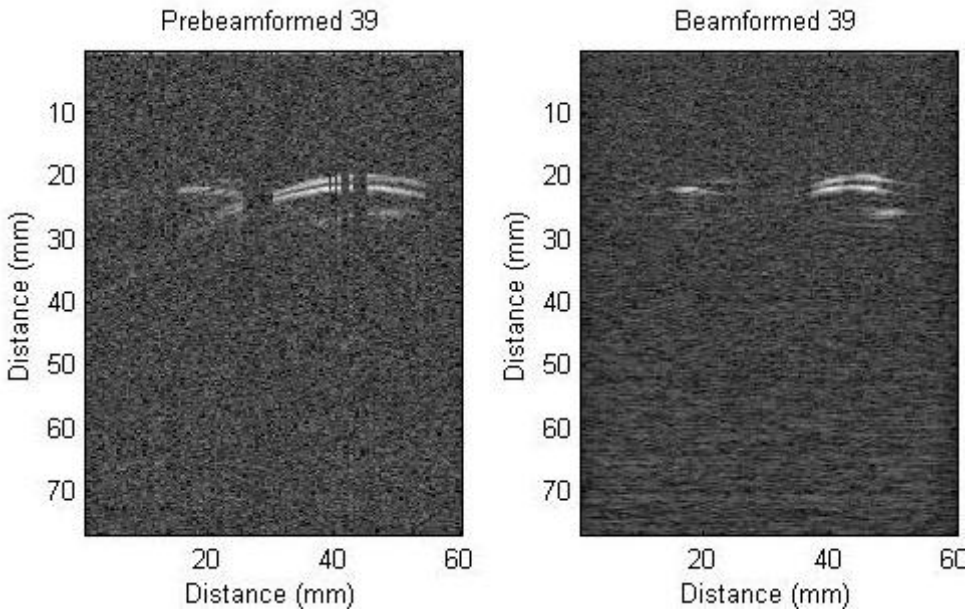

Figure 22: PA image of occlusion and fiber end point at 15mm

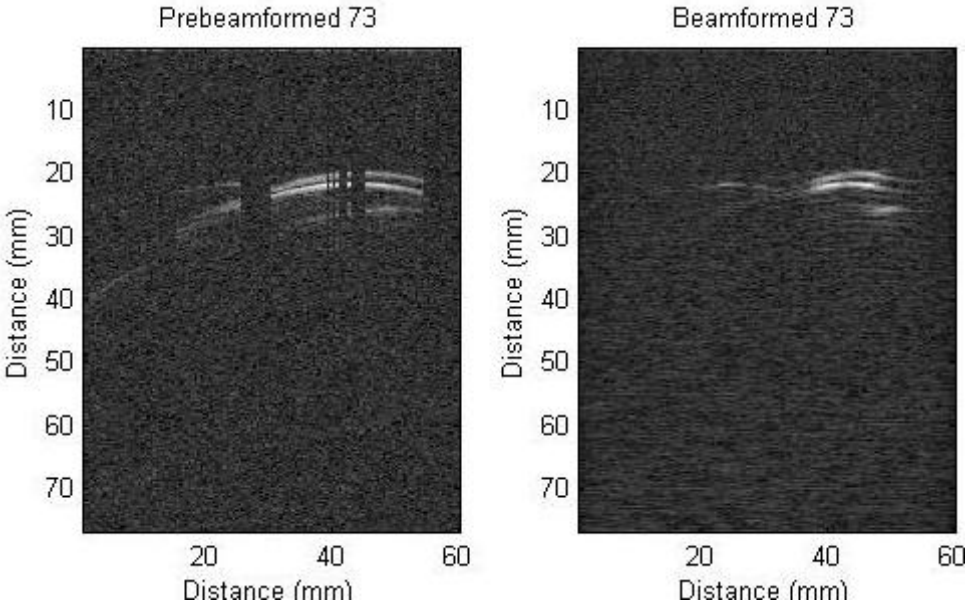

Figure 23: PA image of occlusion and fiber end point at 10mm

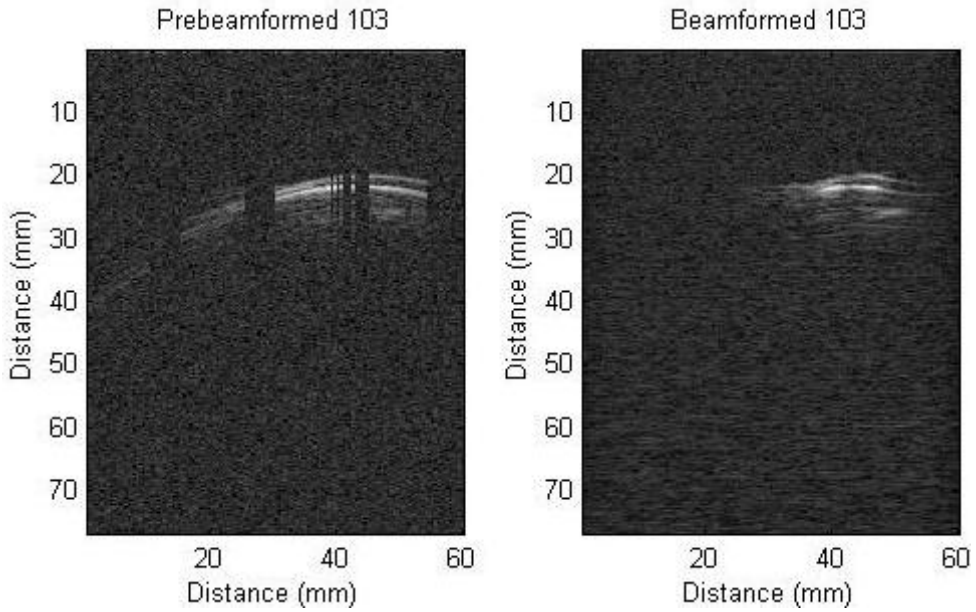

Figure 24: PA image of occlusion and fiber end point at 5mm

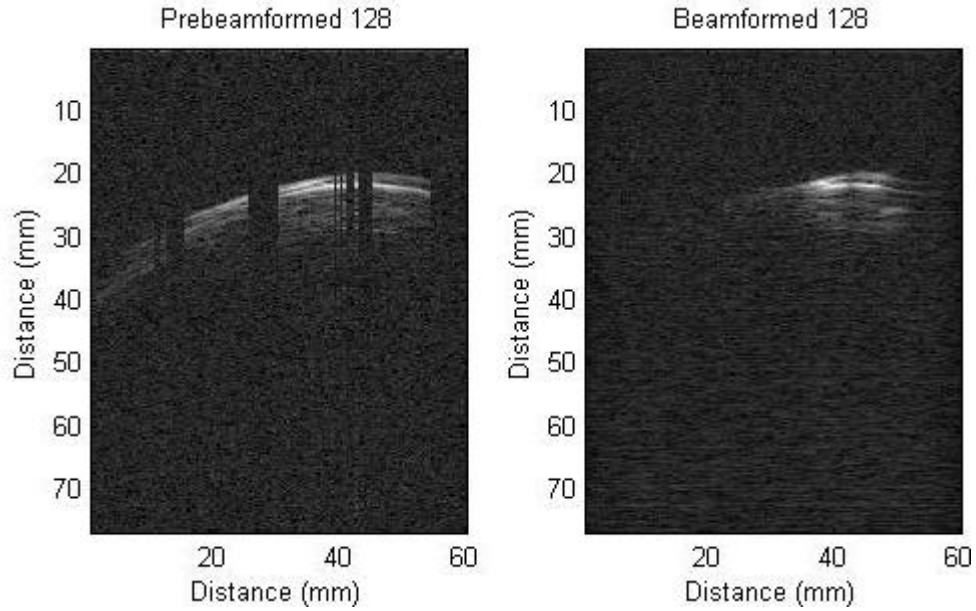

Figure 25: PA image of occlusion and fiber end point at 2mm

Since the seed and the occlusion are really close to each other, the system will recognize their position vertically instead of horizontally, according to their distance to the transducer. As the fiber is approaching, the intensity of the seed and the occlusion is increasing, which corresponds to the previous experiments with the fiber end point distance, while the intensity of the fiber end point is decreasing, due to its relative energy compared to the seed and the occlusion is getting lower.

4. Conclusion

In this project, a new method to image the occlusion in the shunt inside the skull has been proposed and demonstrated with pig pelvis bones of different thickness. Other than transmitting ultrasound waves from the transducer, photoacoustic effect has been adopted to generate the acoustic waves at the occlusion, therefore, the output signal only need to propagate through the skull once and can be detected using an external ultrasound probe. The experiment results show that the signal can be detected and formed into output image with decent resolution to distinguish different levels of occlusions by comparing the size and the contrast of the image. Thus, this method can be used to determine the occlusion and monitor the clearing results for the brain shunt.

As data collecting and processing takes a relatively long time to generate the image, with a maximum speed of 2 frames per second, this technology cannot be used in real-time imaging yet. In the current stage, we can use this method to monitor the clearing procedure for the clearing system in a delayed way. Future research can focus on resolving this limitation by reducing the delays caused by the hardware and software of DAQ, and speeding up the beamforming algorithm in MATLAB. We encourage future researchers to develop new softwares that integrates DAQ, MATLAB and ultrasound system as well. Future experiments with fresh human skull and real occlusion material also need to be conducted to specify the minimum fiber end point energy that can produce image with standard quality. The experiments of visualizing fiber end point with skull also need to be conducted.

5. Management Summary

5.1 Deliverables

All deliverables are achieved though some modifications had to been made during the project. By using the technique we proposed in this project, the occlusion clearing procedure can be monitored in a delayed method using external ultrasound probe. Also, the position and the size of the occlusion can be effectively estimated. The minimum, expected and maximum deliverables are specified below.

Minimum: We built several brain phantoms for the preliminary tests under B-mode and photoacoustic excitation, respectively. The image we got by using the brain phantom without skull demonstrated that the ultrasound system and the photoaoustic Laser System were correctly set up.

Expected: Without changing the system settings, we did the same experiment with different levels of bones and different levels of occlusions. The results in the previous section show that the signals, generated by using photoacoustic excitation, can be detected and collected by the external probe. And by comparing the contrast we can distinguish the occlusion level.

Initially, we also wanted to distinguish shunts, tissues and fluids. According to the setup of this project, laser is directly projecting on the occlusion, so the energy received and reflected by the shunt, tissue and fluid is very low. More over, this energy needs to go through the skull, which causes further attenuation and defocusing. Thus, it is hard to be detected and collected, especially when the effect of defocus exists. Therefore, the experiment results show that they are transparent in the image and can not be distinguished.

Maximum: Initially, we wanted to monitor the clearing procedure in real-time. But this cannot be achieved due to the limitation of both the hardware and the software. Both the DAQ device and MATLAB consume time to collect and process the data, which takes at least 0.5 second to form one image frame. Though this time is really short in daily life, it is still too long for the real-time imaging. Thus, we proposed to monitor clearing process in a delayed method. Also, to conquer the weakness in expected deliverables that we cannot tell the position of the occlusion, we modified the setup to make the relative distance between the fiber end and the occlusion visible, so that we can effectively estimate the position of the occlusion.

5.2 Lessons Learned

In the skull phantom construction part, we used a long time to construct the model in Solidworks and finally found out that the type of 3DP printer is not available in Johns Hopkins University and the 3DP service will miss the best time to do the post-processing. This part of work waste us a really long time though have its own value. The fresh bone we used as our backup plan goes bad easily and certain antiseptic treatment should be made before it is used. Thus, we should check the feasibility of the work in the very starting stage and we should also consider the potential changes in very aspect

before we start.

In addition, this project taught us a detailed plan is good but not enough. The backup plan can play a very key role when we meet the unexpected situation. Timely communication with our advisors can make hard work resolved in a relatively speeded up way.

Acknowledgments

We would like to thank Behnoosh Tavakoli for her help of the system setup and usage training of the ultrasound system and the laser system. We would also like to thank Dr. Boctor and Dr. Taylor for their helpful guidance and financial support throughout the project.

Reference

[1]. Sean Jy-Shyang Chen, Pierre Hellier, Jean-Yvs Gauvrit, Maud Marchal, Xavier Morandi, and D. Louis Collins, An Anthropomorphic Polyvinyl Alcohol Triple Modality Brain Phantom based on Colin27, Mechanical Image Computer-Assisted Intervention – MICCAI 2010 6362 (2010) 92-100.

[2]. Fre´ de´ ric Bevilacqua, Dominique Piguet, Pierre Marquet, Jeffrey D. Gross, Bruce J. Tromberg, and Christian Depeursinge: In vivo local determination of tissue optical properties: applications to human brain. 1 August 1999/ Vol.38, No.22/ Applied Optics.

[3]. Matteo Gatto, Gianluca Memoli, Adam Shaw, Neelaksh Sadhooo, Pierre Gelat, Russell A. Harris, Three-Dimensional Prinrting (3DP) of neonatal head phantom for ultrasound: Thermocouple embedding and simulation of bone, Medical Engineering &Physics 34 (2012) 929-937.